



Some analytical methods for converting thermochronometric age to erosion rate

Sean D. Willett

*Department of Earth Sciences, Swiss Federal Institute of Technology, 8092, Zurich, Switzerland
(swillett@erdw.ethz.ch;)*

Mark T. Brandon

Department of Geology and Geophysics, Yale University, New Haven, Connecticut, USA

[1] An analytical method is presented for converting thermochronometric ages to surface erosion or, equivalently, exhumation rate. The method incorporates the two most important thermal processes during cooling by erosion: the dependence of closure temperature on cooling rate and the advection of heat by rock motion toward the Earth's surface. Two thermal models are considered: (1) a steady state model, valid for low erosion rates; and (2) an eroding half-space model, which has no steady state, but captures the transient increase of geothermal gradient with erosion. In each case, it is assumed that data consist of one or more thermochronometric ages, present-day surface geothermal gradient, and topographic information including the elevation at which the age was obtained. Analytical solutions are provided to derive the erosion rate from these data either as an explicit expression for the steady case or as a root-finding problem for the transient case. A graphical method for plotting age against erosion rate and geothermal gradient is presented as a method for solving the root finding problem and for tracking analytical errors in observations of age and surface geothermal gradient. The graphical method is also appropriate for comparing data from different elevations or from different thermochronometric systems. Examples are provided using synthetic data or published data from the literature.

Components: 7,800 words, 9 figures, 1 table.

Keywords: thermochronometry; thermal model; exhumation.

Index Terms: 1130 : Geomorphological geochronology; 1140 : Thermochronology; 8130 : Heat generation and transport.

Received 6 June 2012; **Revised** 19 November 2012; **Accepted** 30 November 2012; **Published** 31 January 2013.

Willett, S. D., and, M. T. Brandon (2013), Some analytical methods for converting thermochronometric age to erosion rate, *Geochem. Geophys. Geosyst.*, 14, 209–222, doi:10.1029/2012GC004279.

1. Introduction

[2] Thermochronometric dating of a wide assortment of minerals has become a standard tool in the analysis of tectonic, metamorphic, and even geomorphic problems [Bernet *et al.*, 2004; House

et al., 1998; Hurford, 1991; Kamp *et al.*, 1989; Parrish, 1983; Reiners and Brandon, 2006; Reiners *et al.*, 2003; Wagner, 1968; Zeitler, 1985]. Although a thermochronometric age, by definition is a cooling age, its utility is in the interpretation of that cooling age in terms of erosion, which is

defined as surface removal of rock, driving exhumation or motion of the datable mineral toward the surface of the Earth. In either case, the conversion of a thermochronometric age to an erosion rate requires two components: a kinetic model for the dating system in order to calculate the temperature dependence of the closure process, and information about the motion of the dated mineral through the Earth's temperature field, generally through a thermal model.

[3] Thermochronometric systems are defined through a radiogenic parent-daughter relationship, where the daughter is either a radiogenic species or, in the case of fission-track dating, a crystal damage track. The kinetics of the processes vary, and there are many reviews of the various systems [Reiners *et al.*, 2005], but in nearly all cases the temperature dependence of the loss of the daughter product can be expressed through an Arrhenius expression with an activation energy controlling the rate and thus the effective temperature range of daughter loss. With an Arrhenius equation and the simplifying assumption of a constant rate of cooling, Dodson [1973] demonstrated that one can calculate a temperature corresponding to the measured age, which is commonly used as the effective closure temperature.

[4] A wide variety of approaches have been used to model the temperature field in the near surface. For direct interpretation of thermochronometric ages, some approaches include no heat transfer at all, instead inferring a temperature history without specifying an erosion function or explicitly including a heat transfer model [Gallagher *et al.*, 2005]. In other cases, ages are obtained over a range of elevations such that the gradient in age with elevation can be used to directly infer an erosion rate [Brown, 1991; Fitzgerald *et al.*, 1995; Valla *et al.*, 2010]; this method implicitly assumes that temperature is in a steady state. Analytical solutions have also been used to model the temperature field [Brown and Summerfield, 1997; Mancktelow and Grasemann, 1997; Moore and England, 2001], but many of these also use simplifying assumptions, such as steady state, to be practical [Brandon *et al.*, 1998; Stuwe *et al.*, 1994]. Numerical models of heat transfer in one [Ehlers and Farley, 2003; Willett *et al.*, 2003], two [Batt *et al.*, 2000; Braun, 2002; Ehlers *et al.*, 2003; Fuller *et al.*, 2006; Herman *et al.*, 2010], or even three dimensions [Braun, 2003; Herman *et al.*, 2009] have been used to include a range of tectonic kinematic models and to calculate heat transfer by conduction and advection.

[5] In spite of the many complex models available to convert ages to erosion rates [Ehlers *et al.*, 2005], in many cases, a simple analytical expression would be convenient to quickly convert ages to erosion rates. In this paper, we provide a set of such expressions based on analytical solutions for conductive or advective-conductive geotherms in the Earth. These include representations of the two most important physical properties in the system, an expression for closure of the mineral system through a first-order Arrhenius rate equation and upward advection of heat by the erosion process. Our approach is similar to that used by Moore and England [2001], but an important difference is that we include the closure behavior for our estimates of cooling ages.

2. Thermochronometry and the Effective Closure Temperature Concept

[6] Although the kinetics of fission-track annealing or noble gas loss are complex systems and depend on a variety of parameters, to first order they can be treated as Arrhenius processes with an exponential dependence on temperature. First-order kinetics can be expressed in terms of two parameters, an activation energy, E_a , and a frequency factor, Ω . Dodson [1973] demonstrated that the Arrhenius rate equation could be integrated by assuming a constant cooling rate, \dot{T} , to provide parent and daughter concentrations as a function of time. These are used to define the closure temperature of the thermochronometric system as the temperature at the time corresponding to the measured age. Although this is a simplification, and is not valid for complex cooling histories, e.g., reheating with partial resetting, it provides a useful approximation and will be used throughout this paper. Reiners and Brandon [2006] summarized the kinetic parameters for common thermochronometric systems. For convenience, given the long mathematical formulas used through this paper, the gas constant can be combined with the kinetic parameters such that the rate law is expressed in terms of two parameters, A and E

$$A = \frac{\Omega R}{E_a}, E = \frac{E_a}{R}.$$

[7] As discussed in Appendix A, we use an approximate form of Dodson's [1973] expression, which is explicit and depends on the derivative quantity, T_{c10} , defined by Reiners and Brandon [2006] as the closure temperature with a cooling rate of $10^\circ\text{C}/$

Myr. The closure temperature in terms of these quantities can be written as

$$T_c = \frac{E + 2T_{c10}}{2 + \ln(AT_{c10}^2) - \ln(\dot{T})} \quad (1)$$

[8] Equation 1 is an approximation of the Dodson closure temperature expression, but is accurate to within small fractions of a percent and will be used throughout this paper.

3. The Thermal Problem of an Eroding Lithosphere

[9] The concept of a closure temperature greatly simplifies thermal modeling of thermochronometric data. With a closure temperature at a known depth, a thermochronometric age simply corresponds to the time required to move from that closure depth to the surface. The main challenge is to determine the depth to the closure isotherm.

[10] In the sections below, we present some solutions to this problem based on the assumption of one-dimensional, vertical heat transport. The simplest problem that still maintains a self-consistent physical model consists of a thermal calculation based on (1) vertical conduction and advection of heat, (2) a surface temperature condition, and (3) a closure temperature calculated from the cooling rate. The minimum data required for a meaningful calculation of an erosion rate for this case are (1) a measured age, (2) the elevation at which the age was obtained (3) the kinetic parameters, including domain size, for closure of the thermochronologic system, (4) the surface temperature, (5) the topography of the surface in the vicinity of the sampled age, and (6) an estimate of the surface heat flow or geothermal gradient. In any thermochronologic study, all but the last are readily available.

[11] Note that we specify only a single temperature boundary condition here; an alternative formulation would be based on a surface and a lower boundary condition. However, lower boundary conditions are problematic because the only meaningful thermal boundary is at the base of the lithosphere and in most cases, it is difficult to obtain either lithosphere thickness or temperature information. For this reason, many papers assign a fixed temperature at some arbitrary depth, such as the base of the crust. This is not advisable because there is no reason for the base of the crust, or any other point in the lithosphere, to remain isothermal. If the lower boundary condition plays any role, it must be taken

at the base of the lithosphere. An exception might be in the upper plate above subduction zones, where the downgoing plate might hold the base of the fore-arc lithosphere isothermal, but this is a complex two-dimensional problem, which should probably not be treated with one-dimensional models. Fortunately, in many cases, it is not necessary to select any basal boundary condition. Given that the thermal timescale of the lithosphere is on the order of 10^7 Myr, the lower boundary rarely plays any role in perturbations to the near-surface temperature, and if we can characterize the initial or final surface heat flow, the Earth can be treated as infinitely thick, solving the thermal problem for a half-space domain.

[12] The surface heat flow is a measurable quantity and all calculations here will be made with this as a characteristic parameter. If thermal conductivity is homogeneous, the geothermal gradient and the heat flow are equivalent quantities and we will, in fact, use geothermal gradient rather than heat flow for simplicity. In general, geothermal gradient changes with time and depth and we will use the present-day, surface geothermal gradient as the principal parameter in all calculations as this is the measurable quantity. We do not consider the curvature in the geotherm due to radioactive heat generation. This is a linear effect and could be added to the solutions presented here, but for low-temperature systems it has a negligible effect and in all cases it is difficult to constrain independently.

[13] An important characteristic of a half-space domain with surface erosion is that there is no steady state solution. With the time-dependent solutions used here, surface erosion and the resultant heat-advection produce continuously changing surface heat flow and temperature. In spite of this, it can still be useful to assume steady state as an approximation under some conditions and we consider this problem initially.

[14] The surface boundary condition must somehow take into account the roughness of the surface topography as well as the elevation at which an age is obtained [Braun, 2002; Stuwe *et al.*, 1994]. The thermal perturbation due to topography is wavelength-dependent with short wavelength topography having no effect on a given isotherm, whereas an isotherm will parallel long-wavelength topography. The transition from “short” to “long” wavelength is gradual, but occurs at a length scale approximately equal to the depth of the isotherm of interest. In the wave domain, the admittance of surface topography is an exponential function with a

characteristic length of $2\pi z_c$, where z_c is the depth of the closure isotherm [Braun, 2002]. An initial estimate of the depth of the closure isotherm below the mean elevation of the Earth's surface is given as

$$z_c^{\text{est}} = \frac{(T_{c10} - T_0)}{G} \quad (2)$$

[15] An averaging circle with radius of πz_c^{est} thus provides a reasonable basis for averaging the topography and obtaining a mean elevation of the Earth's surface (Figure 1). This elevation is then used as the datum for all thermal calculations including the upper boundary condition, where it is assigned a value of T_0 . The age is given by the time it takes the rock to travel from the closure isotherm to the datum surface, which, in terms of the erosion rate is simply,

$$\tau = \frac{z_c}{\dot{e}}, \quad (3)$$

where \dot{e} is the erosion rate. The case of an age obtained from a rock at an elevation not equal to the mean elevation is discussed later. It remains to determine the value of the closure temperature and its depth, both of which depend on a thermal model.

3.1. Constant, Steady Geothermal Gradient

[16] The simplest possible thermal model is obtained by assuming steady state heat conduction with a negligible advective component, resulting in a geothermal gradient, G , that is constant in depth and time. This is valid only with very low erosion rates or perhaps in a case where kinematics at depth leads to lateral heat flow and a thermal

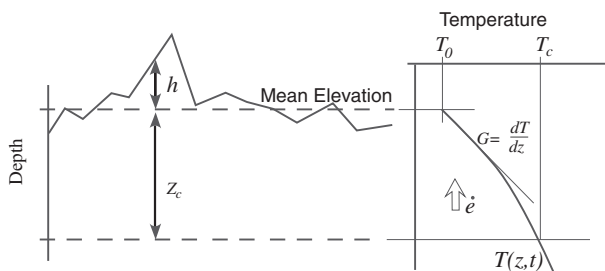


Figure 1. Definitions, boundary conditions, and parameters as used for thermal models in this paper. A geotherm is determined from an average surface elevation, taken at the datum with $z=0$ and with an average surface temperature, T_0 . There is no lower boundary condition, so the geotherm is characterized by the surface gradient, G . The depth from the mean topographic surface to the closure temperature of T_c is z_c .

steady state. The thermochronometric age in terms of temperature can thus be given as

$$\tau = \frac{T_c - T_0}{G\dot{e}} \quad (4)$$

[17] The travel time equation can be combined with the closure temperature expression (equation 1), recognizing that under steady state and a constant geothermal gradient, the cooling rate is simply $G\dot{e}$. Combining equations 1 and 4 with this cooling rate gives the relationship between erosion rate and age

$$\tau G\dot{e} = \frac{E + 2T_{c10}}{[2 + \ln(AT_{c10}^2) - \ln\dot{e} - \ln G]} - T_0 \quad (5)$$

[18] This expression is nonlinear in erosion rate, but after multiplying out the denominator, there are just two difficult terms, $\ln\dot{e}$ and $\dot{e}\ln\dot{e}$, each of which can be linearized using a truncated Taylor series about an arbitrary expansion point. The logical expansion point that we adopt is

$$\dot{e}_a = \frac{T_{c10} - T_0}{G\tau},$$

which gives approximations of

$$\begin{aligned} \ln\dot{e} &\approx \ln\dot{e}_a + \frac{\dot{e} - \dot{e}_a}{\dot{e}_a} \\ \dot{e}\ln\dot{e} &\approx -\dot{e}_a + (1 + \ln\dot{e}_a)\dot{e}. \end{aligned}$$

[19] Substituting these expressions, the erosion rate can be factored out, giving erosion rate as an explicit function

$$\dot{e} = \frac{E + T_{c10} - T_0 \left(\ln\tau + \ln\left(\frac{AT_{c10}^2}{T_{c10} - T_0}\right) + 2 \right)}{\tau G \left[\ln\tau + \ln\left(\frac{AT_{c10}^2}{T_{c10} - T_0}\right) - \frac{T_0}{T_{c10} - T_0} + 1 \right]} \quad (6)$$

[20] Equation 6 is a travel time expression that gives the erosion rate in terms of the surface temperature, the geothermal gradient, and the measured thermochronometric age, but in a form consistent with the cooling-rate dependence of the closure temperature. The Taylor series approximations used to obtain a linear equation are not very restrictive; comparison with numerical solutions of the exact equation shows differences in predicted erosion rate of small fractions of a percent over a wide range of typical ages and erosion rate.

[21] It is interesting that equation 6 has a complex dependence on the age, but the geothermal gradient appears only once, in the denominator. This shows that the estimate of erosion rate depends directly on the geothermal gradient and any uncertainty in G propagates directly into the estimate of the erosion rate.

[22] To illustrate the error propagation from the age and the geothermal gradient, equation 6 can be shown graphically, by plotting erosion rate against geothermal gradient, either on linear or logarithmic axes. In log-log space, an age appears as a line. For example, using the kinetic parameters in Table 1, an apatite fission-track age of 12 Ma and a surface temperature of 7°C gives the graph in Figure 2. A geothermal gradient of 30°C/km predicts an erosion rate of 0.3 km/Myr; an uncertainty of 10°C/km on that geothermal gradient propagates into a range in erosion rate of 0.23 to 0.45 km/Myr. An uncertainty of ±2 Ma in the age extends this range to 0.2 to 0.55 km/Myr as shown in the outer dashed lines in Figure 2. Uncertainty in the kinetic parameters could also lead to uncertainty in the erosion rate estimate, but in most cases, all other sources of error will be small compared to the uncertainty on the geothermal gradient or the error associated with the assumption of a steady, constant gradient.

[23] Other thermochronometric systems can be plotted on the same graph. In fact, given that the slope of an age line is always −1.0 on this graph, any age for any thermochronometer appears as a parallel line. For example, a zircon fission-track of 25.5 Ma, using the kinetic parameters in Table 1 appears identical to the apatite fission track (AFT) age shown in Figure 2. In principle, a plot like Figure 2 is trivial as there is no slope variation and one could reduce all information to a scalar quantity, corresponding to some intercept of the age lines or even just the erosion rate from equation 6, but it remains useful to plot the information in a two dimensional space to illustrate the range and sensitivity to measurement errors, and as is illustrated below, more complex thermal models can also be illustrated on such a $G - \dot{e}$ plot.

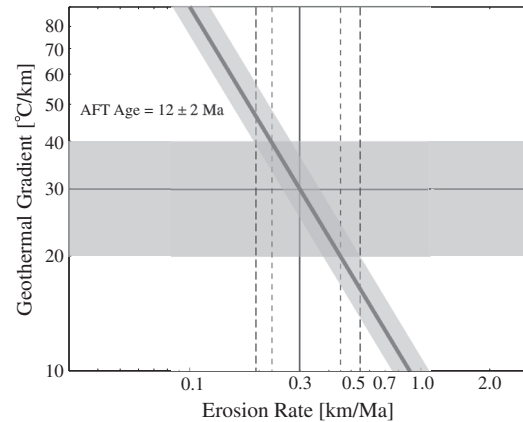


Figure 2. Parametric determination of erosion rate by plotting a thermochronometric age as a function of geothermal gradient and erosion rate through equation 6 with kinetic parameters from Table 1. Erosion rate is determined from the intersection of the observed geothermal gradient and the line representing the age. In this example, an AFT age of 12 Ma and a geothermal gradient of 30°C/km imply an erosion rate of 0.3 km/Ma. Uncertainties (gray areas) in the age and the geothermal gradient imply a range of erosion rate as shown by dashed lines. Note that a zircon fission track age of 25.5 Ma and the corresponding kinetic parameters in Table 1 gives an identical graph.

3.2. Elevation Correction to Constant Geothermal Gradient

[24] In the analysis above, it was assumed that the age came from the surface corresponding to the average elevation. This is not the case in general and if ages are obtained from elevations significantly different from the mean elevation, this will result in variation in the inferred erosion rate. The elevation at which an age is obtained, h , relative to the mean elevation, taken to be positive upward (Figure 1), can simply be added to the travel time, so that the age corresponds to

$$\tau = \frac{z_c + h}{\dot{e}}. \quad (7)$$

[25] Following the same analysis given above, we obtain an erosion rate expression

Table 1. Kinematic Parameters for Example Thermochronometric Systems. From *Reiners and Brandon* [2006]

Thermochronometric System	E_A (kJ/mol)	Ω (s ⁻¹)	T_{c10} (°C)
(U-Th)/He [Farley, 2002]	138	7.64E+07	67
(U-Th)/He [Reiners, 2005]	169	7.03E+05	183
Fission track apatite [Ketcham et al., 1999]	147	2.05E+06	116
Fission track zircon [Brandon et al., 1998]	208	1.00E+08	232

$$\dot{\epsilon} = \frac{E + T_{c10} - (T_0 - hG) \left(\ln \tau + \ln \left(\frac{AT_{c10}^2}{T_{c10} - T_0 + hG} \right) + 2 \right)}{\tau G \left[\ln \tau + \ln \left(\frac{AT_{c10}^2}{T_{c10} - T_0 + hG} \right) - \frac{T_0 - hG}{T_{c10} - T_0 + hG} + 1 \right]} \quad (8)$$

[26] The dependence on geothermal gradient is more complex in this case, but the erosion rate can still be expressed explicitly for a given geothermal gradient. An age can also still be easily plotted in $G - \dot{\epsilon}$ space, although it now appears as a curved function for $h \neq 0$. If multiple ages at different elevations are available, they can all be plotted together in this space. Such a plot has the interesting characteristic that if the ages are colinear in elevation, they imply a constant rate of erosion, and if this rate of erosion is constant to the present day, all ages plot with a common intersection point (Figure 3). In this case, it is not necessary to know the geothermal gradient from independent data, both gradient and erosion rate can be estimated together. However, the estimated geothermal gradient will depend on the datum ($h=0$) selected for the data elevation correction, so this must be selected carefully.

[27] The example in Figure 3 shows the ideal case where a single erosion rate can predict a suite of ages over the time interval of the ages, as well as for the time interval from the youngest age to the present day. It is important to note this last requirement, that the erosion rate has remained constant since closure of the youngest age. This is a major limitation to this approach as it precludes the application to the common situation in which rapid

erosion occurred somewhere in the past, but has not continued to the present day. However, there is a workaround to this limitation as we demonstrate in the natural example at the end of this paper. This method is also not generally an improvement to plotting ages against elevation. In fact, it is worse as far as minimizing the influence of data errors, but it does give additional information regarding the erosion rate over the time interval from the youngest age to the present day. If, however, the age lines do not have a common point, it suggests that the erosion rate has changed at some time between the present day and closure of the oldest sample.

3.3. Temperature in an Exhuming Half-Space

[28] The process of erosion that cools rocks as they move to the Earth's surface also advects heat upward, and thereby changes the geotherm. This effect is significant once erosion rates exceed a few tenths of a millimeter per year. Thus, any internally self-consistent method for calculating cooling ages through erosion should include this transient effect on the depth to the closure isotherm, as well as the aforementioned cooling rate dependence on the closure temperature. Somewhat surprisingly, it is possible to include all these effects in a single analytical approach. Treating the Earth as an infinite half-space with a fixed temperature at the surface and a constant, steady vertical velocity, temperature as a function of depth and time is given by *Carslaw and Jaeger* [1959, p. 388]

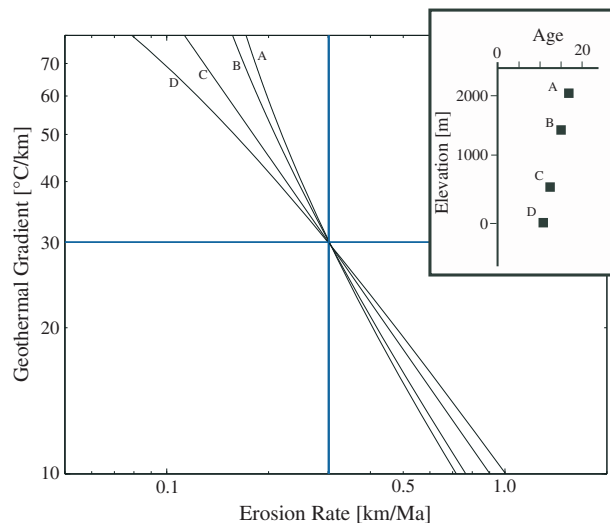


Figure 3. Geothermal gradient, erosion rate plot for four apatite fission track ages using equation 6 and kinetic parameters of Table 1. The ages comprise a linear age elevation profile (inset). The intersection of the age plots gives an erosion rate of 0.3 km/Ma and the geothermal gradient of 30°C/km. Mean elevation (datum) is 1000 m.

$$T = T_0 + G_0 \left\{ (z + \dot{e}t) + \frac{1}{2} \left[(z - \dot{e}t) \exp\left(-\frac{\dot{e}z}{\alpha}\right) \operatorname{erfc}\left(\frac{z - \dot{e}t}{2\sqrt{\alpha t}}\right) - (z + \dot{e}t) \operatorname{erfc}\left(\frac{z + \dot{e}t}{2\sqrt{\alpha t}}\right) \right] \right\}, \quad (9)$$

where α is the thermal diffusivity, G_0 is the initial geothermal gradient, which is taken as constant with depth at time 0, and \dot{e} is the erosion rate, which is taken to be positive in the negative z direction. This solution was applied to thermochronometry data by *Brown and Summerfield* [1997] and analyzed in detail for inverting suites of thermochronometric ages by *Moore and England* [2001]. Note that in this formulation, t is time, not age, running forward from zero at the time of initiation of erosion. Following *Moore and England* [2001], we note that a material point that is at the surface at the present day will have a temperature history determined by setting $z = \dot{e}(t_1 - t)$, where t_1 is the present day relative to the time at which erosion initiated. Restated another way, to be clear, time starts at zero when erosion initiates and runs forward to the present day, reaching this at t_1 . The temperature for a material point at the surface ($z=0$) at the present day ($t=t_1$) as a function of time is

$$T = T_0 + \frac{G_0 \dot{e}}{2} \left\{ (t_1 - 2t) \exp\left(-\frac{\dot{e}^2(t_1 - t)}{\alpha}\right) \operatorname{erfc}\left[\frac{\dot{e}(t_1 - 2t)}{2\sqrt{\alpha t}}\right] - t_1 \operatorname{erfc}\left[\frac{\dot{e}t_1}{2\sqrt{\alpha t}}\right] + 2t_1 \right\}. \quad (10)$$

[29] The cooling rate along this material path is calculated from the time derivative of equation 10 as

$$\frac{dT}{dt} = G_0 \frac{\dot{e}}{2\sqrt{\pi\alpha t}} \left\{ 2\dot{e}t \exp\left(-\frac{t_1^2 \dot{e}^2}{4\alpha t}\right) + \frac{\sqrt{\pi\alpha t}}{\alpha} (2\alpha + (2t - t_1)\dot{e}^2) \exp\left(\frac{(t - t_1)\dot{e}^2}{\alpha}\right) \operatorname{erfc}\left[\frac{(t_1 - 2t)\dot{e}}{2\sqrt{\alpha t}}\right] \right\}. \quad (11)$$

[30] Because we want to calibrate this solution to the modern surface geothermal gradient, we also need the derivative of equation 9 with respect to z , evaluated at $z=0$, giving

$$G = \left. \frac{dT}{dz} \right|_{z=0} = G_0 + \frac{G_0}{2} \left[\frac{2\dot{e}t}{\sqrt{\pi\alpha t}} \exp\left(-\frac{\dot{e}^2 t}{4\alpha}\right) + \frac{\dot{e}^2 t}{\alpha} + \left(2 + \frac{\dot{e}^2 t}{\alpha}\right) \operatorname{erf}\left(\frac{\dot{e}t}{2\sqrt{\alpha t}}\right) \right]. \quad (12)$$

[31] Example solutions of equations 10 and 11 are shown in Figure 4. The geotherm in this case is a function of time and erosion rate, and there is no steady state. As shown in Figure 4, both temperature and cooling rate vary continuously with time. In fact, at long time, the surface geothermal gradient varies approximately linearly with time. It is thus important that we take this time dependence into account for the temperature, but also for the cooling rate and its influence on the closure temperature. Parameters needed for any given solution include the erosion rate, the thermal diffusivity, the initial geothermal gradient, G_0 and the time between the present and the initiation of erosion, which has a magnitude of t_1 .

[32] To predict an age, we need to calculate the closure temperature as a function of depth and time. As in the section above, we will parameterize the

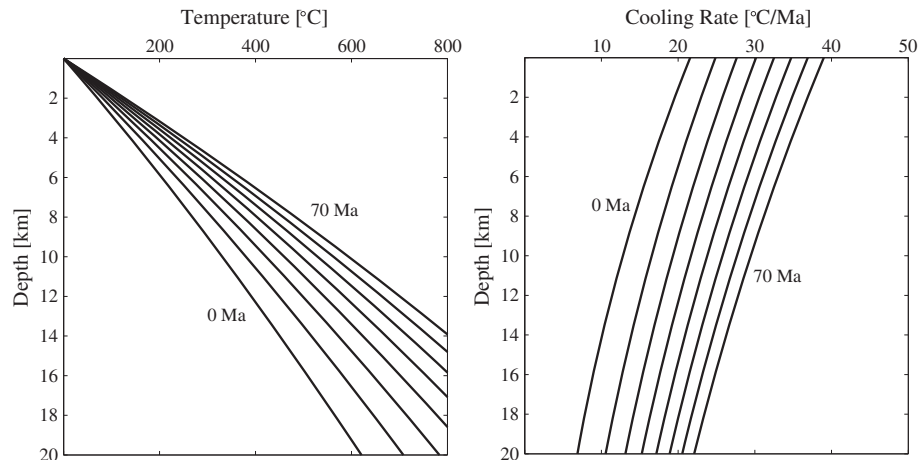


Figure 4. (a) Geotherms for an exhuming half-space as a function of time in 10 Myr steps. Initial gradient is $25^\circ\text{C}/\text{km}$; erosion rate is $0.6 \text{ km}/\text{Ma}$; thermal diffusivity is $32 \text{ km}^2/\text{Ma}$. (b) Material reference frame cooling rates for geotherms in Figure 4a.

problem in terms of the modern surface geothermal gradient. For a given surface geothermal gradient and time since onset of erosion, t_1 , we obtain a suite of geotherms as shown in Figure 5. Closure temperatures are also shown for each geotherm with the closure temperature calculated from equations 1 and 11. An age is calculated by finding the intersection of the geotherm with its corresponding closure temperature, which gives z_c ; the age is simply this depth divided by the corresponding erosion rate.

[33] The inverse problem can also be treated analytically. As with the steady state case discussed previously, we need an estimate of the geothermal gradient; in this case defined to be at the surface at the present day. In addition, we also need to know when erosion initiated, t_1 . It is often possible to estimate this time based on geological information, but if this is not the case and this quantity needs to be guessed, we will show below that results are not strongly sensitive to this parameter. It can also be helpful, and is sometimes possible, to have an estimate of G_0 , the initial geothermal gradient, and

the analysis that follows can easily be modified to express everything in terms of G_0 , rather than G .

[34] Equations 10, 11 and 12 are all complicated functions of t and \dot{e} . To simplify the algebra, we will keep G_0 explicit, but otherwise define functions: F_T , F_R , and F_G , such that equations 10, 11, and 12 can be expressed as

$$T = T_0 + G_0 F_T(t), \quad (13)$$

$$\frac{dT}{dt} = G_0 F_R(t), \quad (14)$$

$$G = G_0 F_G(t) \quad (15)$$

with the functions easily defined by comparison with equations 10, 11, and 12.

[35] Using the cooling rate from equation 14 in the closure temperature expression (equation 1), we obtain a time-dependent closure temperature. We need to equate the temperature from equation 13 to the closure temperature, with both evaluated at the time of closure of the system. For a thermochronometric age of τ , closure occurs at a time of $t_I - \tau$. This is expressed as

$$T_0 + G_0 F_T(t_1 - \tau) = \frac{E + 2T_{c10}}{2 + \ln(AT_{c10}^2) - \ln(G_0 F_R(t_1 - \tau))}. \quad (17)$$

[36] We can eliminate the initial gradient, G_0 , by expressing it in terms of the modern gradient, G , through equation 15 evaluated at t_I , giving

$$T_0 + \frac{G F_T(t_1 - \tau)}{F_G(t_1)} = \frac{E + 2T_{c10}}{2 + \ln(AT_{c10}^2) - \ln G + \ln F_G(t_1) - \ln F_R(t_1 - \tau)}. \quad (18)$$

[37] This is an implicit expression for erosion rate and modern geothermal gradient, and cannot be explicitly solved for \dot{e} , but it is straightforward to find the root with respect to \dot{e} , for example by expressing (18) as,

$$(E + 2T_{c10})F_G(t_1) - (T_0 F_G(t_1) + G F_T(t_1 - \tau)) (2 + \ln(AT_{c10}^2) - \ln G + \ln F_G(t_1) - \ln F_R(t_1 - \tau)) = 0 \quad (19)$$

and, with known values for τ and G , using standard root finding techniques to solve for \dot{e} . There should be a single root for the expression if reasonable bounds for \dot{e} are known.

[38] This can also be solved parametrically using the graphical representation of (18) as a function of G and \dot{e} as was done for the constant gradient case. Solving equation 18 for G , as best we can, we obtain

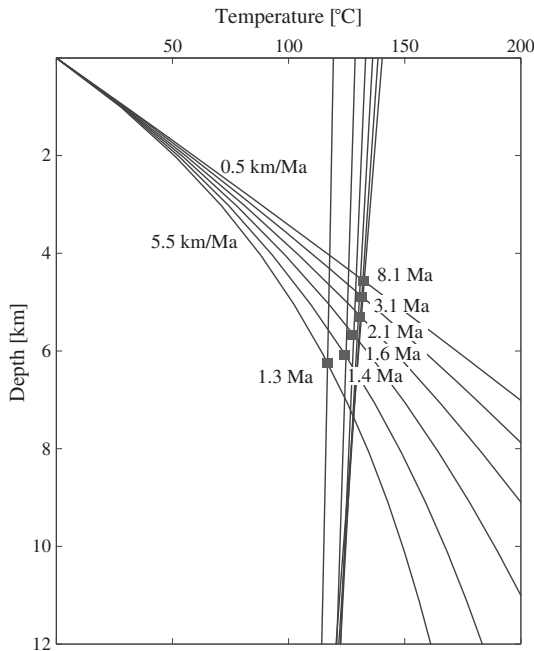


Figure 5. Temperature and AFT closure temperature (near vertical curves) for an exhuming half-space. Erosion rates vary from 0.5 to 5.5 km/Ma in 1.0 km/Ma increments. Duration of erosion is constant at 10 Ma, and initial geothermal gradient is selected so that the final surface geothermal gradient is 30°C/km. Closure temperature varies with cooling rate and thus with depth as indicated. The applicable closure depth is defined by the intersection of the geotherm and its corresponding closure temperature as shown by the square symbols. Ages are determined by travel time from this depth to the surface.

$$G = \frac{(E + 2T_{c10})F_G(t_1)}{F_T(t_1 - \tau)(2 + \ln(AT_{c10}^2) - \ln G + \ln F_G(t_1) - \ln F_R(t_1 - \tau))} \quad (20)$$

$$\frac{T_0 F_G(t_1)}{F_T(t_1 - \tau)}$$

[39] This expression is not quite an explicit relationship between modern gradient (G) and erosion rate, but it is close. There remains one $\ln G$ term on the right side of equation 20. However, $\ln G$ varies little and in practice, G can be determined by direct iteration and converges in just a few iterations. Equation 20 thus gives us an expression for the modern geothermal gradient in terms of a single age, the presumed known kinetic and thermal parameters, a known onset time of erosion, and the unknown erosion rate. As done previously, we can determine the erosion rate graphically by plotting gradient against erosion rate. The same example used in Figure 2, an apatite fission-track age of 12 Ma with a modern geothermal gradient of 30°C/km, is shown in Figure 6. In addition to the previous information we now need to know the onset of erosion, t_1 , which, for this example, we assume to be 30 Ma. The inferred erosion rate is 0.33 km/Myr, close to the 0.3 km/Myr obtained with the assumption of a constant gradient. As with the constant gradient method, the relationship between modern gradient and erosion rate is nearly linear in log-log space, indicating that the inferred erosion rate is very sensitive to the estimate of the modern geothermal gradient. Fortunately, this is not the case for t_1 . Figure 6 shows the same data plotted with t_1 assumed to be 15 Myr and 100 Myr; the inferred erosion rate varies by only

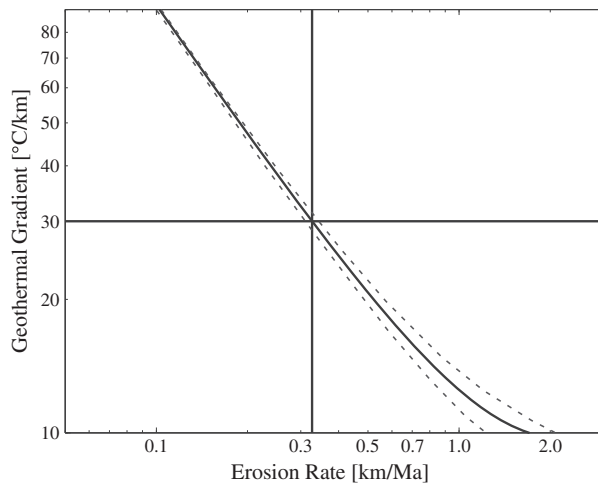


Figure 6. Geothermal gradient, erosion rate plot for an apatite fission track age of 12 Ma, using transient solution of equation 20 and an assumed onset of erosion at 30 Ma. Observed geothermal gradient of 30°C/km implies an erosion rate of 0.33 km/Ma. Dashed lines are for assumed onset of erosion at 15 Ma (upper) and 100 Ma (lower).

a small percentage. However, for other cases, particularly higher erosion rates and the case where the age is close to the onset of erosion, this effect can be larger.

3.4. Elevation Correction to an Exhuming Half-Space

[40] For ages obtained from elevations other than z_m , the temperature history can again be corrected by a simple vertical extension of the cooling path. For an age at an elevation, h , above the mean elevation, i.e., positive is up, even though z is positive down, the temperature history is calculated by substituting $z = \dot{e}(t_1 - t) - h$ in the analysis above. This modifies equations 10 and 11 so that the equivalent functions in equations 13 and 14 become

$$F_T(t) = \frac{1}{2} \left\{ 2\dot{e}t_1 - 2h + (\dot{e}t_1 - 2\dot{e}t - h) \exp\left(-\frac{\dot{e}^2(t_1 - t) - h\dot{e}}{\alpha}\right) \right. \\ \left. \operatorname{erfc}\left[\frac{\dot{e}t_1 - 2\dot{e}t - h}{2\sqrt{\alpha t}}\right] - (\dot{e}t_1 - h) \operatorname{erfc}\left[\frac{\dot{e}t_1 - h}{2\sqrt{\alpha t}}\right] \right\} \quad (21)$$

$$F_R(t) = \frac{\dot{e}}{2\sqrt{\pi\alpha t}} \left\{ 2\dot{e}t \cdot \exp\left(-\frac{(t_1\dot{e} - h)^2}{4\alpha t}\right) \right. \\ \left. + \frac{\sqrt{\pi\alpha t}}{\alpha} (2\alpha + \dot{e}(h + 2\dot{e}t - t_1\dot{e})) \exp\left(\frac{h\dot{e} + (t - t_1)\dot{e}^2}{\alpha}\right) \right. \\ \left. \operatorname{erfc}\left[\frac{(t_1 - 2t)\dot{e} - h}{2\sqrt{\alpha t}}\right] \right\}. \quad (22)$$

[41] As an example, three ages generated using the half-space solution are plotted in $G - \dot{e}$ space in Figure 7. The data are error free and were generated with an erosion rate of 0.5 km/Myr and thus plot with a single crossing point, reproducing perfectly the underlying erosion rate and the modern geothermal gradient. The 4 km of relief used for this example is admittedly extreme, but serves to emphasize the changing form of the age functions. Note that these data are not collinear in age-elevation space, as the closure isotherm is not constant with time.

4. Example: Denali Massif Fission-Track Data

[42] As an example as to how this analysis can be used, we use a suite of data taken from the literature [Fitzgerald *et al.*, 1995]. This suite of data contains 15 fission-track ages, distributed over nearly 4 km of elevation (Figure 8). The elevation range is important as it permits the gradient in age with elevation to be used to directly infer erosion rate and therefore test our solution. The ages (Figure 8) show a well defined increase in age with elevation, including a break in the slope that can be

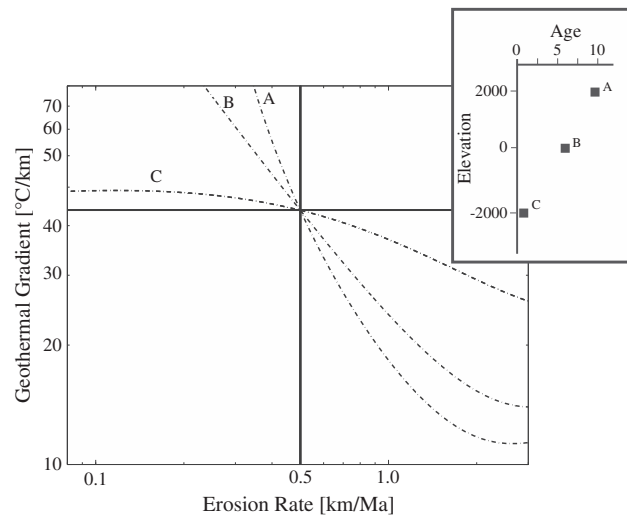


Figure 7. Model-generated ages distributed over 4 km of elevation difference (inset) and plotted in $G - \dot{e}$ space according to equations 20, 21, and 22, and assuming the onset of erosion at 15 Ma. The erosion rate and present-day geothermal gradient are recovered exactly by the intersection point of the three curves. Depth of zero is defined to be at the mean topography for the problem.

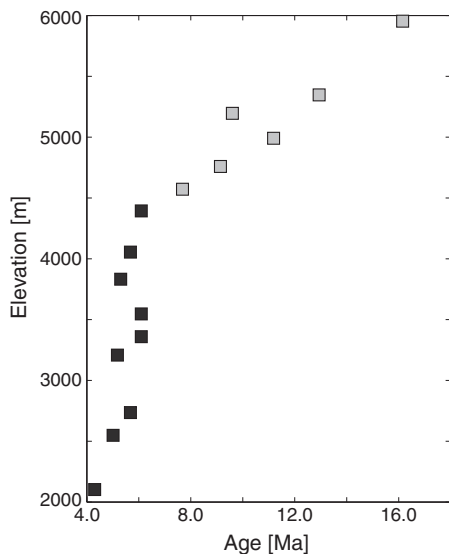


Figure 8. Apatite fission-track ages from the Denali Massif, taken from Fitzgerald *et al.* [1995], as a function of sampled elevation. Black and grey points are modeled separately and shown in Figure 9.

interpreted as representing a change in erosion rate. The Denali region has the disadvantage that we know little about the heat flow or geothermal gradient of the region, but the redundancy provided by the large number of ages allows us to independently estimate the geothermal gradient.

[43] The two slopes in the age, elevation data imply a change in erosion rate which violates the assumptions of the analytical solutions, but we can analyze the ages that cooled during each erosion phase. The

younger ages (black points in Figure 8) represent the most recent cooling that we assume has continued to the present day. As such we can use equation 20 with the functions of equations 15, 21, and 22, to transform each age into a function in geothermal gradient (modern), erosion rate space. We need an upper boundary condition which we take as a temperature of -10°C at the mean elevation, which we estimate at 3.5 km above sea level. We use the kinetic parameters from Table 1 and assume an onset of erosion at 6.5 Ma. Using equation 20 with these data yields the result shown in Figure 9a. In principle, all age functions should have a common crossing point, but in practice there is scatter in the ages (Figure 8) resulting from analytical error and physical processes. However, the age functions do converge in an area supporting an erosion rate in the range of 0.65 to 1.2 mm/yr and a modern geothermal gradient of 30 to $35^{\circ}\text{C}/\text{km}$. The inverse gradient of age with elevation for these data is 1.2 mm/yr but as Fitzgerald *et al.* [1995] noted, this is likely too high due to heat advection and they estimated an erosion rate of 0.9 to 1.1 mm/yr, similar to our estimate. They also noted the lack of thermal data to constrain this calculation, but estimate a geothermal gradient above $30^{\circ}\text{C}/\text{km}$. A lower gradient would fit the data equally well and would imply a higher erosion rate, but a geothermal gradient below $30^{\circ}\text{C}/\text{km}$ is unlikely for a region with prolonged tectonic activity and erosion.

[44] The older, higher elevation ages can also be analyzed by our method, although only with some modification. We need to apply the thermal solution for conditions at 6.5 Ma, directly following the

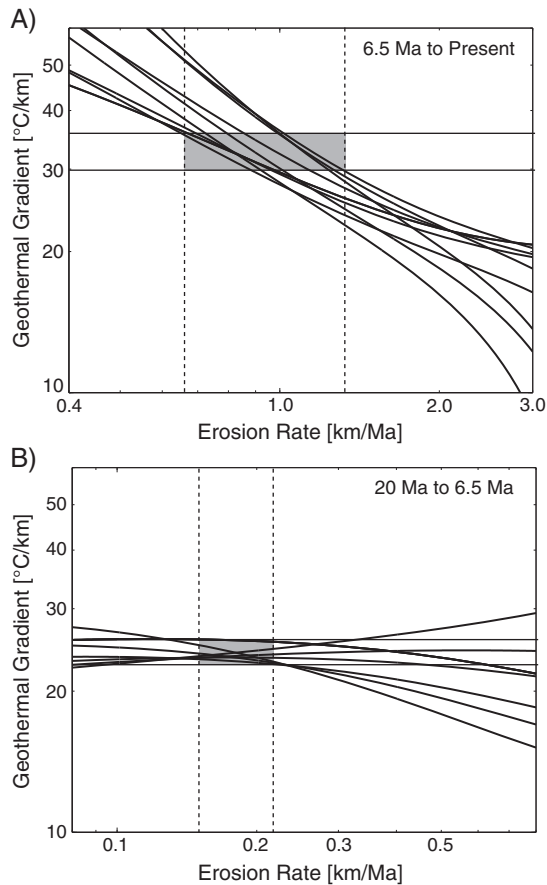


Figure 9. Geothermal gradient, erosion rate plots for fission track ages shown in Figure 8. (a) Lower elevation samples shown in black in Figure 8. These were modeled assuming an onset of erosion 6.5 Ma and using the half-space solution. A present-day geothermal gradient of 30 to 35°C/km implies an erosion rate of 0.65 to 1.2 km/Ma, consistent with all data. Kinetic parameters from Table 1 were used. (b) Model for the high-elevation samples shown in grey on Figure 8. Erosion was assumed to be active at this rate from 20 Ma to 6.5 Ma. A geothermal gradient of 22 to 28°C/km at 6.5 Ma and an erosion rate of 0.15 to 0.21 km/Ma are inferred.

period of slower erosion, but before the period of rapid erosion. To correct the data back to this age, we take the mean erosion rate from the analysis above (0.9 mm/yr) and reduce the elevation of all the ages by this times 6.5 Ma. We are thus restoring 5.9 km of erosion. We also reduce each age by 6.5 Ma. These modified age, elevation pairs can then be transformed into gradient, erosion rate functions as we did above. Results are in Figure 9b. These data converge nicely to a single point in gradient, erosion rate space, with the exception of one age, which is somewhat of an outlier for its elevation (age of 9.3 Ma at 5.3 km). Otherwise, the ages suggest an erosion rate of just under

0.2 mm/yr and a geothermal gradient at 6.5 Ma of 25°C/Myr. This geothermal gradient matches the initial gradient used for the analysis of the ages from 6.5 Ma to the present.

5. Discussion and Conclusions

[45] The analysis presented here provides a simple method for converting thermochronometric ages to erosion rate. The more general, transient solution includes the two physical phenomena that must be present for thermochronometric ages that are set during erosional cooling: advection of heat by the erosion process and the cooling rate dependence of the closure temperature. The significance of the method presented here is that these phenomena can be included in simple analytical expressions; any of the solutions presented here can be implemented with just a few lines of code (Appendix B).

[46] The analysis also demonstrates the minimum data needed for even a minimalistic calculation: a thermochronometric age with the kinetic information for calculating closure of the system and an estimate of the present-day geothermal gradient. Secondary information includes the surface topography in the vicinity of a measured age, surface temperature, and duration of erosion prior to the present. Although these latter quantities can often be estimated roughly, any estimate of erosion rate depends directly on the present-day geothermal gradient and the accuracy of the estimate is as sensitive to the geothermal gradient as it is to the measured age.

[47] This sensitivity to geothermal gradient can be demonstrated and assessed through a simple graphical exercise of plotting an age against geothermal gradient and erosion rate through one of the expressions derived here. This serves not only to provide an estimate of the erosion rate at a given geothermal gradient, solving the root-finding problem inherent to the transient solution, but also shows graphically how error propagates into the erosion rate estimate, by plotting the range of age or of geothermal gradient (e.g., Figure 2). This graphical tool is also useful to show data from different elevations or from different mineral systems to test for internal self-consistency.

[48] The largest limitation of the method is the requirement that the erosion rate must be constant from the time of closure to the present day. This is a stricter requirement than that of age-elevation plots that resolve erosion rate directly over the measured age range. Given that erosion rate should

be constant until the present day, the expressions derived here are best applied to active tectonic environments where erosion is on-going.

[49] This restriction can be avoided in some cases. For example, if one can reconstruct the erosion history in steps such that the youngest erosion steps are estimated, the ages can be analyzed by incremental application of the expressions derived above. We demonstrated this process in the example from Alaska. However, we violate some of our assumptions through this process. For example, the assumption of a linear initial geotherm is not consistent with stepwise erosion. At some point, it is simply easier to use a numerical model, and these analytical expressions will be limited in application.

[50] In conclusion, this method, although not of universal application, should provide a useful tool for age interpretation. The inclusion, in a self-consistent manner, of a cooling-rate dependent closure temperature with an exhuming half-space thermal model captures the essential physics of the thermal processes, and remains simple enough for easy application without the use of simplistic assumptions such as steady state or arbitrary fixed-temperature boundary conditions.

Appendix A

[51] *Dodson* [1973] considered a system where the loss of a daughter product was temperature-dependent through a first-order rate equation, and where the inverse temperature evolved on a monotonic cooling path which can be approximated by a constant cooling rate, \dot{T} . Under these conditions, the daughter, parent ratio defining the age corresponds to a single temperature, T_c , which defines the closure temperature. *Dodson* expressed this as an implicit relationship in terms of the closure temperature

$$\dot{T} = AT_c^2 \exp\left(-\frac{E}{T_c}\right), \quad (\text{A.1})$$

where T_c is the closure temperature and A and E are the kinetic parameters as defined in the main body of this paper. It would be convenient to invert equation A.1 to obtain an explicit expression for T_c , but this is not possible. However, by linearizing the expressions using truncated Taylor series expansions, we can obtain an approximate solution. giving T_c explicitly. By transforming the temperature variable:

$$T^* = \frac{I}{T}$$

and taking the logarithm of equation A.1, we obtain

$$\ln(\dot{T}) = \ln(A) - 2\ln(T_c^*) - ET_c^*. \quad (\text{A.2})$$

[52] This has a near linear form and thus the Taylor series approximation is more accurate. *Reiners and Brandon* [2006] used $10^\circ\text{C}/\text{Myr}$ rate as a typical geologic cooling rate and tabulated values of T_c for various thermochronometric systems using this cooling rate and equation A.1. This makes this a convenient expansion point, which we refer to as T_{c10} .

[53] The transformed expansion point is thus $T_{c10}^* = 1/T_{c10}$, and the Taylor-series approximation for the logarithmic term is

$$\ln(T_c^*) \approx \ln(T_{c10}^*) + \frac{1}{T_{c10}^*} (T_c^* - T_{c10}^*).$$

[54] Substituting this back into (A.2), we obtain an expression linear in T_c^* . Solving this and inverting gives us an explicit expression for closure temperature as a function of cooling rate

$$T_c = \frac{E + 2T_{c10}}{2 + \ln(AT_{c10}^2) - \ln(\dot{T})}. \quad (\text{A.3})$$

[55] Although equation A.3 is an approximation, the Arrhenius rate equation on which equation A.1 is close to linear in log time, inverse temperature space, so this approximation is imperceptible over several orders of magnitude. For kinematic parameters other than those given by *Reiners and Brandon* [2006], it is necessary to solve (A.1) for T_{c10} using $\dot{T} = 10$.

Appendix B

[56] Matlab script for solving for erosion rate from a thermochronometric age. This script solves the exhuming half-space problem (equations 13, 14, 15, 20, 21, and 22).

```
% calculates the erosion rate from the modern gradient and an age
% This is an exact inversion of the half-space solution in depth and time
% based on Willett and Brandon, G-cubed
% set the parameters here
% t1 - duration (age of onset) of erosion before present (Ma)
% tau = observed age (in Ma)
% T0 = surface temperature (in kelvin) at mean elevation
% Gobs = an estimate of the modern geothermal gradient (deg C/km)
% Gobs2 = a second estimate of the modern geothermal gradient (use both estimates to provide bounds)
% h = elevation of sample above mean elevation (km)
t1=35.69;
T0=5+273;
h=2.0;
tau=9.87;
Gobs=43.72;
Gobs2=43.72;
% pick a thermochron system (copy 5 lines to bottom of list)
% zircon Tagami
omega=1.64e14*3.1557e13;
ea=324000;
tc10=338+273;
isys=1;
% He Reiners
omega=7.03e5*3.1557e13;
```

```

ea=169000.;
tcl0=183.+273.;
isys=2;

%Alto Farley
omega=7.64e7*3.1557e13;
ea=139000.;
tcl0=67+273;
isys=4;

%Zircon Brandon
omega=1.0e08*3.1557e13;
ea=209000.;
tcl0=32+273;
isys=1.;

%apatite ft ketcham
omega=2.05e6*3.1557e13;
ea=147000.;
tcl0=116+273;
isys=3;

% set u vector to search
% bounds can't be too broad or some functions blow up
% this depends on the age and t1
% also used as plotting bounds
%
umin=-08;
umax=2.;

% set plot bounds on gradient
gmin=10.;
gmax=70.;

% set some other things
r=8.314472;
d=log(omega*r/ea);
E=ea/r;
alpha=32.;
u=logspace(log10(umin), log10(umax), 1000);

% modern gradient FG function
% Willett and Brandon eqn (12) evaluated at present day (t1)
t=t1*ones(size(u));
FG=1+.5*(2*u.*t.*exp(-
u.*t./(4*alpha))./sqrt(pi*alpha*t)+u.*t./alpha+(2*u.*t./alpha).*erf(u.*t./(2*sqrt(alpha*t)))));

% Temperature FT function Evaluated at time of closure (t1=tau)
% Willett and Brandon Eqn (21)
t=(t1-tau)*ones(size(u));
FT=(2*u.*t1-2*h+(u.*t1-2*u.*t-h).*exp(-(u.*t1-t-h.*u)/alpha)).*erfc((u.*t1-2*u.*t-h)
./((2*sqrt(alpha*t1)))-(u.*t1-h).*erfc((u.*t1-h)./(2*sqrt(alpha*t1)))/2);

% cooling rate F function Evaluated at time of closure (t1=tau)
% Willett and Brandon Eqn (22)
FDot=sqrt(pi*alpha*t1).*(2*alpha+u.*(h+2*t.*u-t1*u)/alpha).*erfc(((t1-2*t1)*u-h)./(2*sqrt(alpha*t1)));
FDot=FDot.*exp((h./u+t-t1).*u.^2/alpha);
FDot=FDot*2*u.*t.*exp((-t1.*u-h).^2./(4*alpha*t1));
FDot=FDot.*u./((2*sqrt(pi*alpha*t1)));

% iterate 5 times for G non-linear term
G=Goba*ones(size(u));
for i=1:5
    G=(E+2*tcl0)*FG./((E+2*log(tcl0)+2*log(G)+log(FG)-log(FDOT)))-T0.*FG./FT; % geothermal gradient
end

a=G./FG; % find initial geothermal gradient - not used but interesting to check sometimes
% find the roots or intersections of erosion rate from gradient estimates
flag=0;
for i=1:999
    if G(i) > Goba
        if G(i+1) < Goba
            if flag == 0
                uGoba=u(i)+(Goba-G(i))/(G(i+1)-G(i))* (u(i+1)-u(i))
                flag=1;
            end
        end
    end
end
flag=0;
for i=1:999
    if G(i) > Goba2
        if G(i+1) < Goba2
            if flag == 0
                uGoba2=u(i)+(Goba2-G(i))/(G(i+1)-G(i))* (u(i+1)-u(i))
                flag=1;
            end
        end
    end
end

% Set some line endpoints for plotting
Gline1(1)=Goba;
Gline1(2)=Goba;
Gline1x(1)=.0001;
Gline1x(2)=100.;
Gline2y(1)=Goba2;
Gline2y(2)=Goba2;
Gline2x(1)=.0001;
Gline2x(2)=100.;
uline1(1)=.0001;
uline1(2)=500.;
uline1x(1)=uGoba;
uline1x(2)=uGoba;

% chance to plot different systems with different lines or colors
if isys==1
    loglog(u,G,'k',Gline1x,Gline1y,'k', Gline2x,Gline2y,'k',uline1x,uline1y,'k',uline2x,uline2y,'k')
end
if isys == 2
    loglog(u,G,'k',Gline1x,Gline1y,'k', Gline2x,Gline2y,'k',uline1x,uline1y,'k',uline2x,uline2y,'k')
end
if isys==3
    loglog(u,G,'k-',Gline1x,Gline1y,'k', Gline2x,Gline2y,'k',uline1x,uline1y,'k',uline2x,uline2y,'k')
end
if isys==4
    loglog(u,G,'--k',Gline1x,Gline1y,'k', Gline2x,Gline2y,'k',uline1x,uline1y,'k',uline2x,uline2y,'k')
end

set(findobj('Type','axes'),'Box','on','FontSize',18)
set(findobj('Type','line'),'LineStyle','solid')
xlabel('Erosion Rate [km/Ma]')
ylabel('Geothermal Gradient [°C/km]')
axis([umin umax gmin gmax])

```

References

Batt, G. E., J. Braun, P. Kohn Barry, and I. McDougall (2000), Thermochronological analysis of the dynamics of the Southern Alps, New Zealand, *Geol. Soc. Am. Bull.*, *112*(2), 250–266. doi:10.1130/0016-7606.

Bernet, M., M. T. Brandon, J. I. Garver, and B. Molitor (2004), Fundamentals of detrital zircon fission-track analysis for provenance and exhumation studies with examples from the European Alps, in *Detrital Thermochronology: Provenance analysis, exhumation, and landscape evolution of Mountain belts* edited by M. Bernet and C. Speigal, pp. 25–36, Geological Society of America, Boulder, Colorado.

Brandon, M., M. Roden-Tice, and J. Garver (1998), Late Cenozoic exhumation of the Cascadia accretionary wedge in the Olympic Mountains, northwest Washington State, *Geol. Soc. Am. Bull.*, *110*(8), 985–1009. doi:10.1130/0016-7606.

Braun, J. (2002), Estimating exhumation rate and relief evolution by spectral analysis of age-elevation datasets, *Terra Nova*, *14*(3), 210–214. doi:10.1046/j.1365-3121.2002.00409.x.

Braun, J. (2003), Pecube: a new finite-element code to solve the 3D heat transport equation including the effects of a time-varying, finite amplitude surface topography, *Comput. Geosci.*, *29*(6), 787–794. doi:10.1016/S0098-3004(03)00052-9.

Brown, R. W. (1991), Backstacking apatite fission-track “stratigraphy: A method for resolving the erosional and isostatic rebound components of tectonic uplift histories, *Geology*, *19*, 74–77. doi:10.1130/0091-7613.

Brown, R., and M. Summerfield (1997), Some uncertainties in the derivation of rates of denudation from thermochronologic data, *Earth Surf. Processes Landforms*, *22*(3), 239–248. doi:10.1002/(SICI)1096-9837(199703)22:3<239::AID-ESP751>3.0.CO;2-B.

Carlsaw, H. S., and J. C. Jaeger (1959), *Conduction of Heat in Solids*, 2nd Edn., Oxford University Press, Oxford.

Dodson, M. H. (1973), Closure Temperature in Cooling Geochronological and Petrological Systems, *Contrib. Mineral. Petrol.*, *40*(3), 259–274.

Ehlers, T. A., and K. A. Farley (2003), Apatite (U-Th)/He thermochronometry: methods and applications to problems in tectonic and surface processes, *Earth Planet. Sci. Lett.*, *206*(1-2), 1–14. doi:10.1016/S0012-821X(02)01069-5.

Ehlers, T. A., Chaudhri, T., Kumar, S., Fuller, C., Willett, S. D., Ketcham, R., Brandon, M. T., et al. (2005). Computational tools for low-temperature thermochronometer interpretation. *Low-Temp. Thermochronol.: Tech., Interpret., Appl.*, *58*(1), 589–622. doi:10.2138/rmg.2005.58.22.

Ehlers, T. A., S. D. Willett, P. A. Armstrong, and D. S. Chapman (2003), Exhumation of the central Wasatch Mountains, Utah: 2. Thermokinematic model of exhumation, erosion, and thermochronometer interpretation, *J. Geophys. Res.-Solid Earth*, *108*(B3). doi:10.1029/2001JB001723.

Farley, K. A. (2002), (U-Th)/He dating: Techniques, calibrations, and applications, *Rev. Mineral. Geochem.*, *47*, 819–844. doi:10.2138/rmg.2002.47.18.

Fitzgerald, P. G., Sorkhabi, R. B., Redfield, T. F., and Stump, E. (1995). Uplift and denudation of the central Alaska Range: A case study in the use of apatite fission track thermochronology to determine absolute uplift parameters. *J. Geophys. Res.*, *100*(B10), 20175–20191. doi:10.1029/95JB02150.

Fuller, C. W., S. D. Willett, D. Fisher, and C. Y. Lu (2006), A thermomechanical wedge model of Taiwan constrained by fission-track thermochronometry, *Tectonophysics*, *425*(1-4), 1–24. doi:10.1016/j.tecto.2006.05.018.

Gallagher, K., J. Stephenson, R. Brown, C. Holmes, and P. Fitzgerald (2005), Low temperature thermochronology and modeling strategies for multiple samples 1: Vertical profiles, *Earth Planet. Sci. Lett.*, *237*(1-2), 193–208. doi:10.1016/j.epsl.2005.06.025.

Herman, F., Copeland, P., Avouac, J. P., Bollinger, L., Mahéo, G., Le Fort, P., Rai, S., et al. (2010). Exhumation, crustal deformation, and thermal structure of the Nepal

- Himalaya derived from the inversion of thermochronological and thermobarometric data and modeling of the topography. *J. Geophys. Res.*, *115*(B6), B06407. doi:10.1029/2008JB006126.
- Herman, F., S. C. Cox, and P. J. J. Kamp (2009), Low-temperature thermochronology and thermokinematic modeling of deformation, exhumation, and development of topography in the central Southern Alps, New Zealand, *Tectonics*, *28*(5), TC5011. doi:10.1029/2008TC002367.
- House, M. A., B. P. Wernicke, and K. A. Farley (1998), Dating topography of the Sierra Nevada, California, using apatite (U-Th)/He ages, *Nature (London)*, *396*(6706), 66–69. doi:10.1038/23926.
- Hurfurd, A. (1991), Uplift and Cooling Pathways Derived From Fission-Track Analysis and Mica Dating - a Review, *Geologische Rundschau*, *80*, 349–368. doi:10.1007/BF01829371.
- Kamp, P. J. J., P. F. Green, and S. H. White (1989), Fission track analysis reveals character of collisional tectonics in New Zealand, *Tectonics*, *8*, 169–195.
- Ketcham, R. A., R. A. Donelick, and W. D. Carlson (1999), Variability of apatite fission-track annealing kinetics: III. Extrapolation to geological timescales, *Am. Mineral.*, *84*, 1235–1255.
- Mancktelow, N. S., and B. Grasemann (1997), Time-dependent effects of heat advection and topography on cooling histories during erosion, *Tectonophysics*, *270*, 167–195. doi:10.1016/S0040-1951(96)00279-X.
- Moore, M., and P. England (2001), On the inference of denudation rates from cooling ages of minerals, *Earth Planet. Sci. Lett.*, *185*(3–4), 265–284.
- Parrish, R. R. (1983), Cenozoic thermal evolution and tectonics of the Coast Mountains of British Columbia I. Fission-track dating, apparent uplift rates, and patterns of uplift, *Tectonics*, *2*, 601–631.
- Reiners, P. (2005), Zircon (U-Th)/He thermochronometry. *Low-Temp. Thermochronol.: Tech., Interpret., Appl.*, *58*, 151–179.
- Reiners, P. W., and M. T. Brandon (2006), Using thermochronology to understand orogenic erosion, *Annu. Rev. Earth Planet. Sci.*, *34*, 419–466. doi: 410.1146/annurev.earth.1134.031405.125202.
- Reiners, P. W., T. A. Ehlers, S. G. Mitchell, and D. R. Montgomery (2003), Coupled spatial variations in precipitation and long-term erosion rates across the Washington Cascades, *Nature*, *426*(6967), 645–647.
- Reiners, P., T. Ehlers, and P. Zeitler (2005), Past, present, and future of thermochronology, *Low-Temp. Thermochronol.: Tech., Interpret., Appl.*, *58*, 1–18.
- Stuwe, K., L. White, and R. Brown (1994), The influence of eroding topography on steady-state isotherms. Applications to fission track analysis, *Earth Planet. Sci. Lett.*, *124*, 63–74.
- Valla, P. G., F. Herman, P. A. Van Der Beek, and J. Braun (2010), Inversion of thermochronological age-elevation profiles to extract independent estimates of denudation and relief history — I: Theory and conceptual model, *Earth Planet. Sci. Lett.*, *295*(3–4), 511–522. doi:10.1016/j.epsl.2010.04.033.
- Wagner, G. A. (1968), Fission-track dating of apatites, *Earth Planet. Sci. Lett.*, *4*, 411–415.
- Willett, S. D., D. Fisher, C. Fuller, Y. En-Chao, and C. Y. Lu (2003), Erosion rates and orogenic-wedge kinematics in Taiwan inferred from fission-track thermochronometry, *Geology*, *31*(11), 945–948. doi:10.1130/G19702.1.
- Zeitler, P. K. (1985), Cooling history of the Himalaya, Pakistan, *Tectonics*, *4*, 127–151. doi:10.1029/TC004i001p00127.